Eur. Phys. J. A (2016) **52**: 171
DOI 10.1140/epja/i2016-16171-5

THE EUROPEAN PHYSICAL JOURNAL A

Regular Article – Theoretical Physics

Ranking and validation of the spallation models for description of intermediate mass fragment emission from p + Ag collisions at 480 MeV incident proton beam energy

Sushil K. Sharma[1], Bogusław Kamys[1,a], Frank Goldenbaum[2], and Detlef Filges[2]

[1] The Marian Smoluchowski Institute of Physics, Jagiellonian University, Łojasiewicza 11, 30-348 Kraków, Poland
[2] Institut fuer Kernphysik, Forschungszentrum Juelich, 52425 Juelich, Germany

Received: 11 February 2016 / Revised: 5 May 2016
Published online: 24 June 2016

Communicated by T. Duguet

Abstract. Double-differential cross-sections $d^2\sigma/d\Omega\, dE$ for isotopically identified intermediate mass fragments (^{6}Li up to ^{27}Mg) from nuclear reactions induced by 480 MeV protons impinging on a silver target were analyzed in the frame of a two-step model. The first step of the reaction was described by the intranuclear cascade model INCL4.6 and the second one by four different models (ABLA07,GEM2, GEMINI++, and SMM). The experimental spectra reveal the presence of low-energy, isotropic as well as high-energy, forward-peaked contributions. The INCL4.6 model offers a possibility to describe the latter contribution for light intermediate mass fragments by coalescence of the emitted nucleons. The qualitative agreement of the model predictions with the data was observed but the high-energy tails of the spectra were significantly overestimated. The shape of the isotropic part of the spectra was reproduced by all four models. The GEM2 model strongly underestimated the value of the cross-sections for heavier IMF whereas the SMM and ABLA07 models generally overestimated the data. The best quantitative description of the data was offered by GEMINI++, however, a discrepancy between the data and the model cross-sections still remained for almost all reaction products, especially at forward angles. It indicates that non-equilibrium processes are present which cannot be reproduced by the applied models. The goodness of the data description was judged quantitatively using two statistical deviation factors, the H-factor and the M-factor, as a tool for ranking and validation of the theoretical models.

1 Introduction

It is well known for proton-induced reactions that the qualitative properties of the spectra and angular distributions of the spallation products indicate the presence of two different processes [1–12]. One of them contributes to low-energy part of the spectra (energy range smaller than 30–50 MeV), has evaporative-like character and therefore produces isotropic angular distributions. Another mechanism results in forward-peaked angular distributions, is associated to pre-equilibrium processes and participates to a much broader energy range of the ejectiles. The question remains: what are the additional reaction mechanisms responsible for the obvious discrepancies of data and considered models? The idea behind modeling the physics picture of the process generally assumes that the protons of GeV energies induce an intranuclear cascade of two-body nucleon-nucleon collisions since the average distance between nucleons in the nucleus is larger than the dimensions of the wave packet ($\sim$ 1 fm) representing the impinging proton. Such a cascade is a non-equilibrium process which could result in anisotropic emission of fast particles. In the early models of intranuclear cascade (INC) only nucleons and eventually pions are emitted leaving behind a residuum of the target in an excited state. In newer models other processes were introduced to allow for the emission of particles composed of several nucleons. Recently a new version of the INC model has been invented, INCL4.6 [13], which is able to describe the emission of IMF (intermediate mass fragments, *i.e.* particles heavier than ^{4}He but lighter than fission products) by the process of surface coalescence. The model takes into account the ejectiles with mass number up to $A = 12$. It was demonstrated [13] that this model coupled with the ABLA evaporation-fission model [14], reproduces well a large set of observables (total reaction cross-sections, neutron, proton, pion, and composite double-differential cross-sections, neutron multiplicities, residue mass and charge distributions, and

[a] e-mail: ufkamys@cyf-kr.edu.pl

residue recoil velocity distributions) for reactions induced by protons of a broad range of energies (from 0.2 to 2 GeV) on Fe, Ni, Au and Pb targets. The aim of the present work is to investigate the quality of the data reproduction by the INCL4.6 model [13] coupled to four different models describing the second stage of the reaction: ABLA07 [14], GEMINI++ [15, 16], GEM2 [17, 18] and SMM [19–22] for a silver target which has the mass number intermediate between those of lighter Fe, Ni on the one hand and heavier Au, Pb targets on the other hand. The data of Green *et al.* [5] have been taken for this purpose because they contain double-differential cross-sections $\mathrm{d}^2\sigma/\mathrm{d}\Omega\,\mathrm{d}E$ measured at several scattering angles between 10° and 160° (laboratory system) for isotopically identified intermediate mass fragments of 10 elements from Li to Mg: ^{6,7,8,9}Li, ^{7,9,10,11}Be, ^{8,10,11,12,13}B, ^{11,12,13,14}C, ^{14,15,16,17}N, ^{15,16,17,18,19}O, ^{17,18,19,20,21,22}F, ^{20,21,22,23}Ne, ^{22,23,24,25,26}Na, ^{24,25,26,27}Mg. These data were obtained in experiments in which a silver target was bombarded by a proton beam of the energy of 480 MeV. The experimental spectra of Green *et al.* reveal unambiguously a presence of two components called by the authors "evaporative" and "non-evaporative" contributions. Such a rich set of experimental data enables one i) to test whether the coalescence mechanism present in the INCL4.6 is able to reproduce the high-energy "non-evaporative" spectra of lightest IMF, and ii) to check whether the data for heavier IMF also need an inclusion of such a process.

Results of calculations performed by means of the intranuclear cascade INCL4.6 [13] ("non-evaporative" contribution) coupled to four different models of the second stage of the reaction are presented in sect. 2. They are compared with experimental cross-sections allowing for a qualitative judgement on the importance of different reaction mechanisms. The quantitative agreement between the model and experimental cross-sections is also discussed using the values of two statistical deviation factors (the H-factor and the M-factor) as a criterion allowing for validation and ranking of the applied models.

Results of the qualitative and quantitative comparison are summarized in the last section.

2 Analysis of $\mathrm{d}^2\sigma/\mathrm{d}\Omega\mathrm{d}E$ cross-sections

The theoretical analysis of the data was performed using the approach of a two-step model. The INCL4.6 computer code of Boudard *et al.* [13] was used to describe the first step of the reaction. This code which uses the Monte Carlo method allows for the emission of nucleons and pions as well as the emission of composite particles with mass number up to $A = 12$. However, as it is emphasized by Boudard *et al.* [13] the computing time increases extremely fast with the maximal mass of the emitted cluster due to increase of the combinatorics of emission of different particles. Therefore the authors of INCL4.6 consider in their paper only composite particles with $A < 9$. We followed this procedure and performed the high statistics calculations for composite particles with $A < 9$. To check stability of calculations in respect to assumed maximal mass of the emitted cluster, sample calculations with smaller statistics have been also done assuming maximal cluster mass $A < 11$. It turned out that the results for $A = 8$, *i.e.* the heaviest cluster in high statistics calculations are overestimated significantly (by a factor $\approx$ 6–7) as was pointed out by Boudard *et al.* However values of the cross-sections for emission of lighter particles, their energy and angular distributions are negligibly affected as is also the case for heavy residual nuclei.

In the second step the de-excitation of the target remnant was calculated by means of four different models. It should be emphasized that different mechanisms of the de-excitation are realized by each of these models.

The generalized evaporation model (GEM2) by Furihata [17, 18] includes sequential evaporation of particles evaluated according to formalism of Weisskopf and Ewing [23], and it allows for fission of the excited nucleus in accordance with Atchison's [24] fission model.

The ABLA07 statistical model [14] describes the de-excitation process of the thermalised nucleus in terms of particle evaporation, nuclear multifragmentation and fission. If the excitation energy per nucleon of the nucleus exceeds a limiting value (default 4.2 MeV/nucleon) then the simultaneous break-up of the nucleus appears. For smaller excitation energies the de-excitation of the nucleus proceeds through sequential evaporation and/or fission.

The same processes are taken into account by the SMM model [19–22], however, with different prescriptions to incorporate them into the calculations. SMM assumes that the de-excitation process proceeds in two steps. In the first step, the equilibrated excited target's remnant expands within a fixed freeze-out volume, which is defined as a volume in which the nuclear interaction between fragments vanishes and the fragments experience only the mutual Coulomb field. Then the nucleus breaks up into nucleons and hot fragments. All break-up channels allowed by conservation laws are taken into consideration. The formation of the compound nucleus and its de-excitation via evaporation or fission processes is considered as one of the possible channels. Thus the transition from evaporation at low excitation energies to fragmentation at high energies is decided on the basis of the available phase space.

The GEMINI++ model was developed by Charity [15, 16] to describe the nuclear de-excitation as a series of sequential binary decays (no multi-fragmentation allowed strictly). It uses different formalisms: 1) the Hauser-Feshbach formalism [25] for very asymmetric decays, *i.e.*, for emission of neutrons, light charged particles and light intermediate mass fragments, 2) the Bohr-Wheeler formalism [26] for symmetric fission of very heavy systems and 3) the Moretto generalized transition-state formalism [27] for other decays.

Parameters of all the models were fixed during the calculations at values proposed by authors of the models and no attempt was undertaken to adjust them for better description of the data. This enabled us to judge qualitatively the predictive power of the models. Furthermore, it allows to make the validation and ranking of the models.

In the first step of the analysis the qualitative agreement of the experimental and theoretical cross-sections was taken into consideration.

The representative data (dots) and theoretical cross-sections (lines) determined at four laboratory angles (20, 60, 90, and 120 degrees) are presented in figs. 1–5. For IMF with mass number not larger than $A = 8$ the sums of the INCL4.6 cross-sections and the cross-sections of corresponding four models of the second stage of the reaction are shown. For heavier ejectiles only results of the models describing the second step of the reaction are depicted.

The presence of the exponential tail of the spectra, extended to high energies is clearly seen for all scattering angles of the Li and Be data presented in fig. 1. This effect is also pronounced at forward hemisphere of scattering angles for B as well as for angles 20° and 60° for C cross-sections as shown in fig. 2. In the case of boron and carbon ejectiles the theoretical coalescence contribution is absent because all these IMF have mass number larger than eight: $A > 8$. The strong underestimation of high-energy data by the model calculations calls for the need of an inclusion of some additional non-equilibrium, high-energy contribution. The situation becomes more complicated for IMF with $Z \geq 7$ as is discussed below.

It should be pointed out that the coalescence contribution evaluated by means of the INCL4.6 does not properly reproduce the experimental spectra of light IMF, *i.e.* ^{6,7,8}Li and ^{7}Be. The exponential tail of theoretical spectra is always too flat what leads to an overestimation of data at energies larger than ~ 80 MeV for ^{6,7}Li and ^{7}Be and at all energies for ^{8}Li.

In case of elements with $Z \geq 7$ the theoretical spectra evaluated by models of the second stage of the reaction reproduce reasonably well the shape of the experimental spectra. It should be, however, noticed that the agreement between the data and model cross-sections varies from angle to angle. This means that the experimental angular distributions are not isotropic as it is predicted by the theoretical models based on the assumption of the equilibration of the excited nucleus emitting the IMF. Therefore also the non-equilibrium contribution cannot be neglected for IMF with $Z \geq 7$.

The cross-sections evaluated by the GEM2 model always significantly underestimate the data. The difference becomes so large (more than two orders of magnitude) for ^{20,21}F, ^{23}Ne as well as for all isotopes of Na and Mg that the theoretical cross-sections of this model are not shown in figs. 4 and 5, respectively. In conclusion, one can state that GEM2 cannot be used for a reasonable description of the data discussed in the present work. On the contrary, the GEMINI++ model gives the best agreement for spectra of N, O, F, Ne, Na and Mg isotopes presented in figs. 3–5. This agreement is nevertheless not satisfactory for forward scattering angles of all N, O, F isotopes as well as of ^{21}Ne-^{23}Ne, ^{24}Na-^{25}Na isotopes (cf. figs. 3, 4 and 5). There the experimental spectra are underestimated. This may point to the presence of some contribution in the data from the non-equilibrium processes which is expected to be the largest for small scattering angles.

The ABLA07 and SMM spectra for F, Ne, Na and Mg isotopes overestimate the data. The agreement improves for forward scattering angles. At these angles a contribution of non-equilibrium processes may be present. Therefore the data which may contain contributions from equilibrium and non-equilibrium processes agree apparently with model cross-sections of ABLA07 and SMM which produce too large cross-sections. In the case of GEMINI++ the underestimation of data at forward angles can be explained in the same context, *i.e.*, by the presence in the data the non-equilibrium contribution mentioned above. Thus it shows that the GEMINI++ gives the best estimation of the equilibrium processes.

Besides the qualitative comparison of the data and model calculations the following procedure of quantitative analysis has been applied: First, the statistical factors which are proposed in the literature for quantitative judgement of the agreement of the data and theoretical cross-sections were calculated. The results allowed us to validate the models, *i.e.* to state whether the description of the data is satisfactory. Then this condition has been relaxed and only the relative quality of the data description has been studied to obtain a ranking of the applied models.

In the literature, many statistical tests were proposed and used to judge the data description by different models [28]. All tests calculate the deviation factors which quantitatively determine the magnitude of the difference between the measured and theoretical cross-sections. This difference is usually weighted by the experimental errors or by the experimental cross-sections theirselves. To validate the model one has to know the value of the deviation factors which corresponds to the perfect agreement between the model and experimental cross-sections. Since the data are always affected by statistical errors, the perfect agreement has to be understood as the equality of expectation values of the data with the model cross-sections. If the theoretical cross-sections are calculated by the Monte Carlo method one has to take also into consideration the statistical spread of theoretical values [29].

In the present study we use two deviation factors, the H-factor [28] and the M-factor [29], which for a large number of cross-sections (*i.e.* asymptotically) behave like the normal random variables with known expectation values and standard deviations:

$$H \equiv \left[\frac{1}{N}\sum_{i=1}^{N}\left(\frac{\sigma_i^{\mathrm{exp}} - \sigma_i^{\mathrm{cal}}}{\Delta_i}\right)^2\right]^{1/2}, \tag{1}$$

$$M \equiv \frac{1}{N}\sum_{i=1}^{N}\left|\frac{\sigma_i^{\mathrm{exp}} - \sigma_i^{\mathrm{cal}}}{\Delta_i}\right|, \tag{2}$$

$$\Delta_i \equiv \sqrt{\left(\Delta\sigma_i^{\mathrm{exp}}\right)^2 + \left(\Delta\sigma_i^{\mathrm{cal}}\right)^2},$$

where σ_i^{exp}, $\Delta\sigma_i^{\mathrm{exp}}$, and σ_i^{cal}, $\Delta\sigma_i^{\mathrm{cal}}$ are the i-th experimental cross-section, its error and the corresponding model ("calculated") cross-section and its error, respectively.

Subtracting the expectation value of each deviation factor and dividing the result by its standard deviation one obtains the standardized normal random variable which

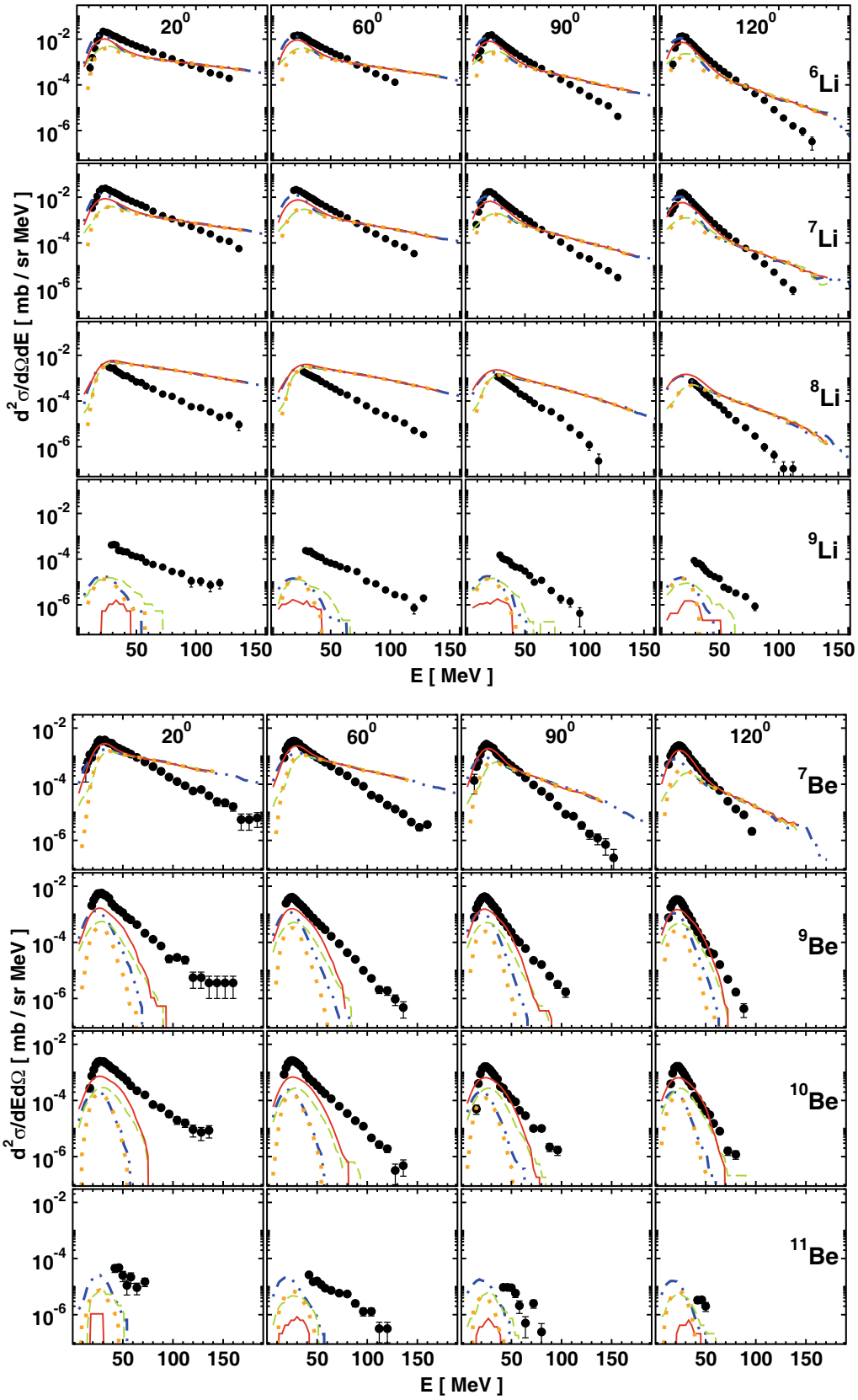

Fig. 1. Experimental (dots) and theoretical (lines) spectra for isotopes of Li (upper four panels) and Be (lower four panels) emitted at four different angles: 20, 60, 90, and 120 degrees (columns from left to right). The lines: solid (red), dashed (green), dash-dotted (blue) and dotted (yellow) correspond to SMM, ABLA07, GEMINI++ and GEM2, respectively.

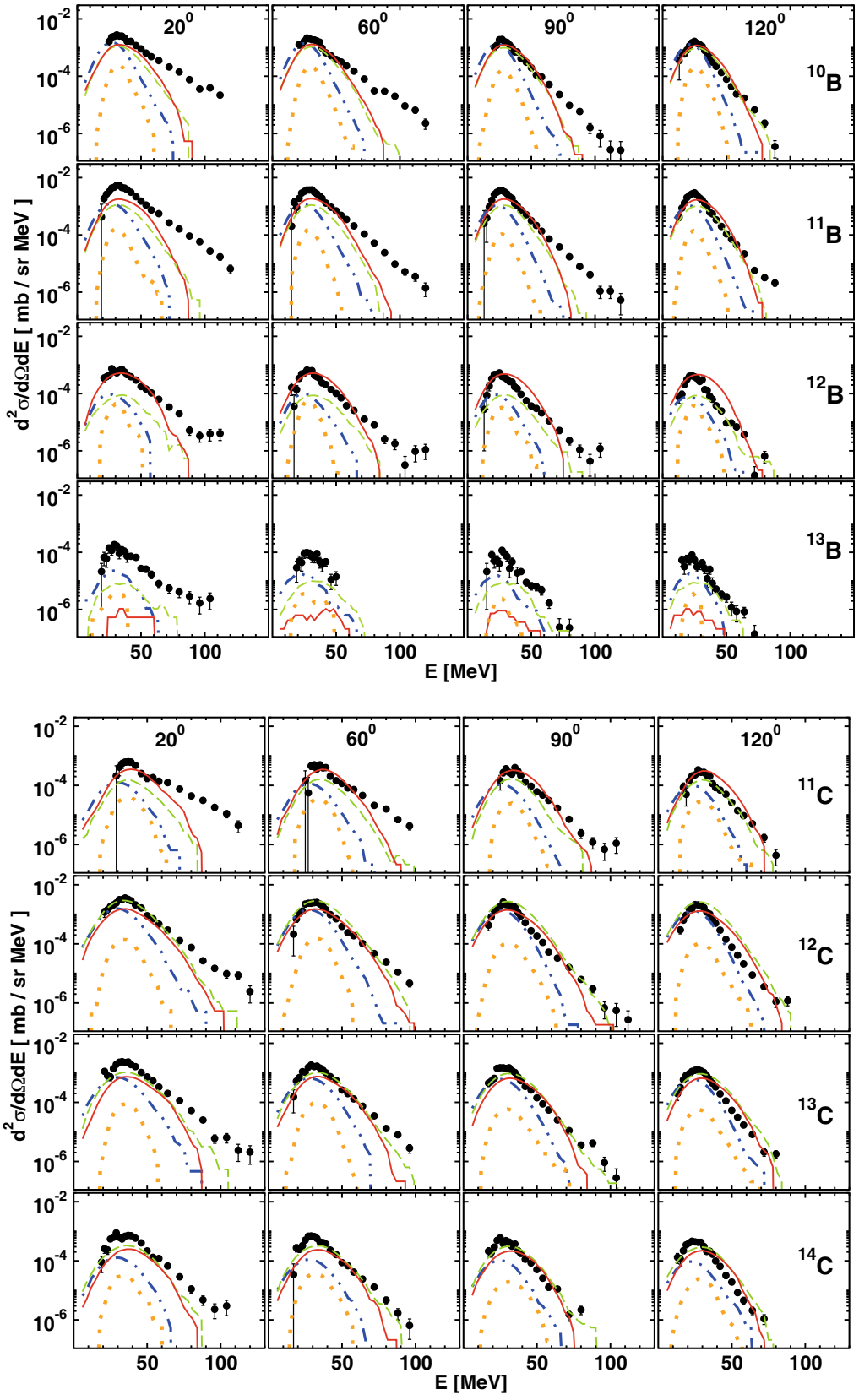

Fig. 2. Experimental (dots) and theoretical (lines) spectra for isotopes of B (upper four panels) and C (lower four panels) emitted at four different angles: 20, 60, 90, and 120 degrees (columns from left to right). The lines: solid (red), dashed (green), dash-dotted (blue) and dotted (yellow) correspond to SMM, ABLA07, GEMINI++ and GEM2, respectively.

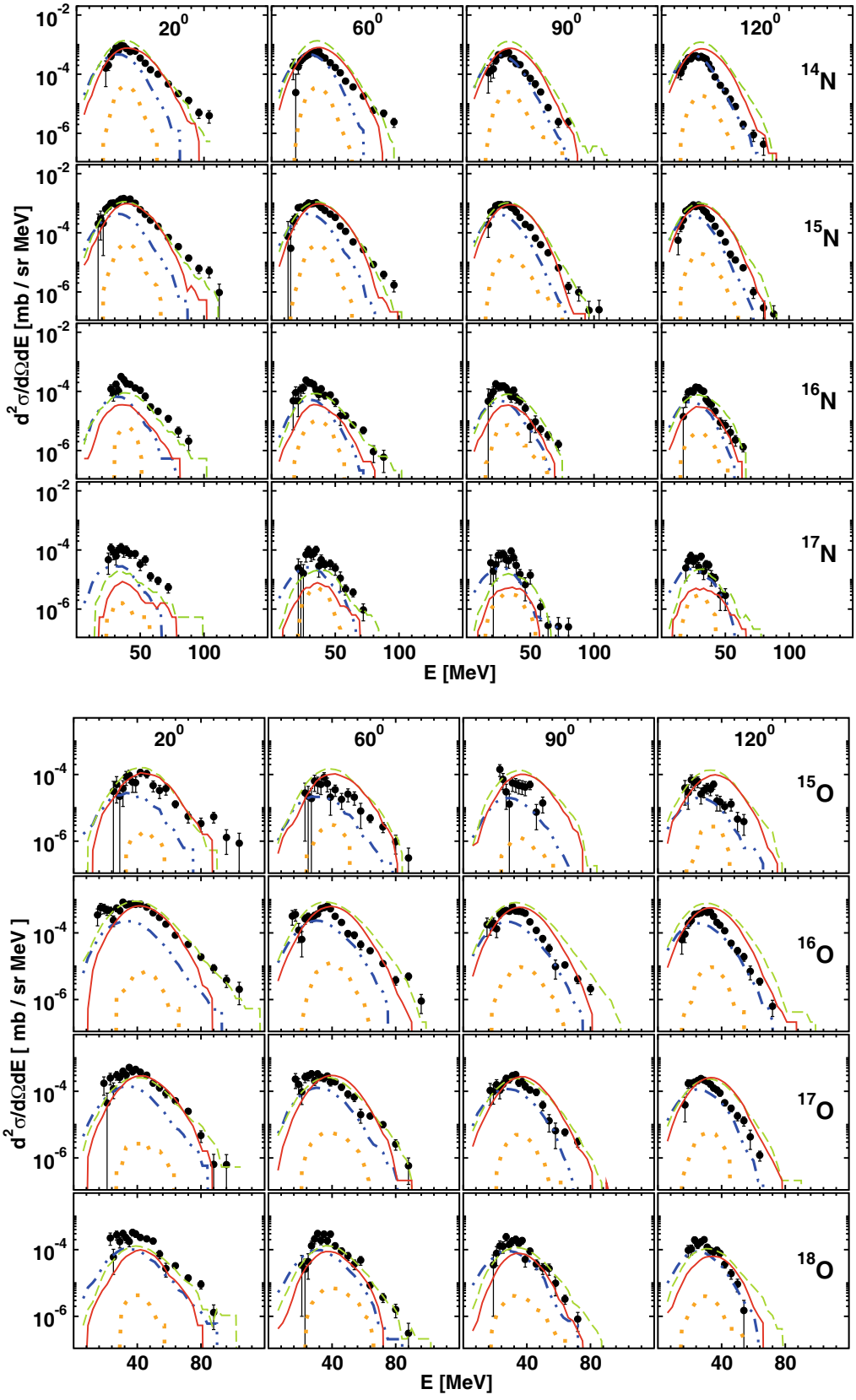

Fig. 3. Experimental (dots) and theoretical (lines) spectra for isotopes of N (upper four panels) and O (lower four panels) emitted at four different angles: 20, 60, 90, and 120 degrees (columns from left to right). The lines: solid (red), dashed (green), dash-dotted (blue) and dotted (yellow) correspond to SMM, ABLA07, GEMINI++ and GEM2, respectively.

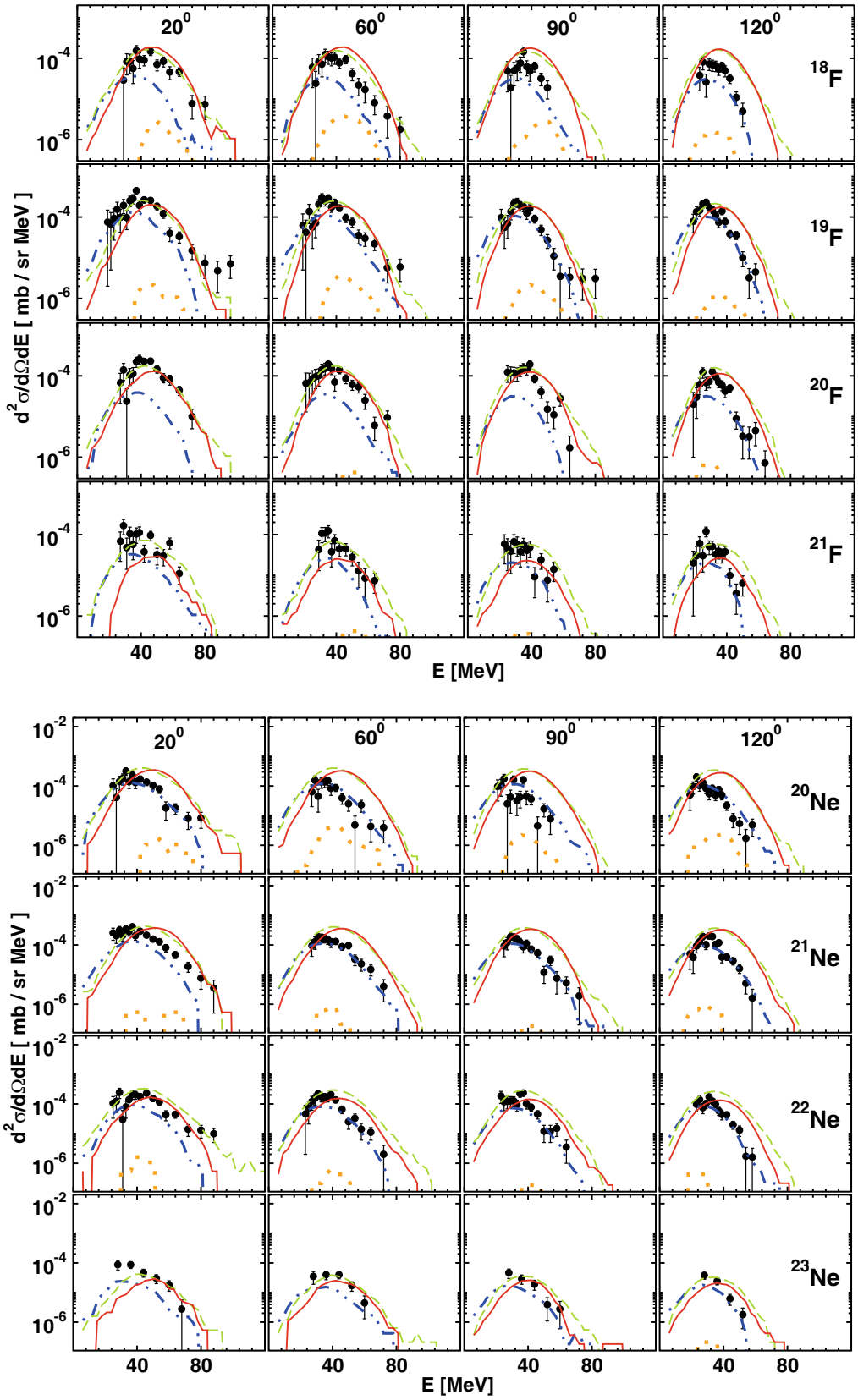

Fig. 4. Experimental (dots) and theoretical (lines) spectra for isotopes of F (upper four panels) and Ne (lower four panels) emitted at four different angles: 20, 60, 90, and 120 degrees (columns from left to right). The lines: solid (red), dashed (green), dash-dotted (blue) and dotted (yellow) correspond to SMM, ABLA07, GEMINI++ and GEM2, respectively.

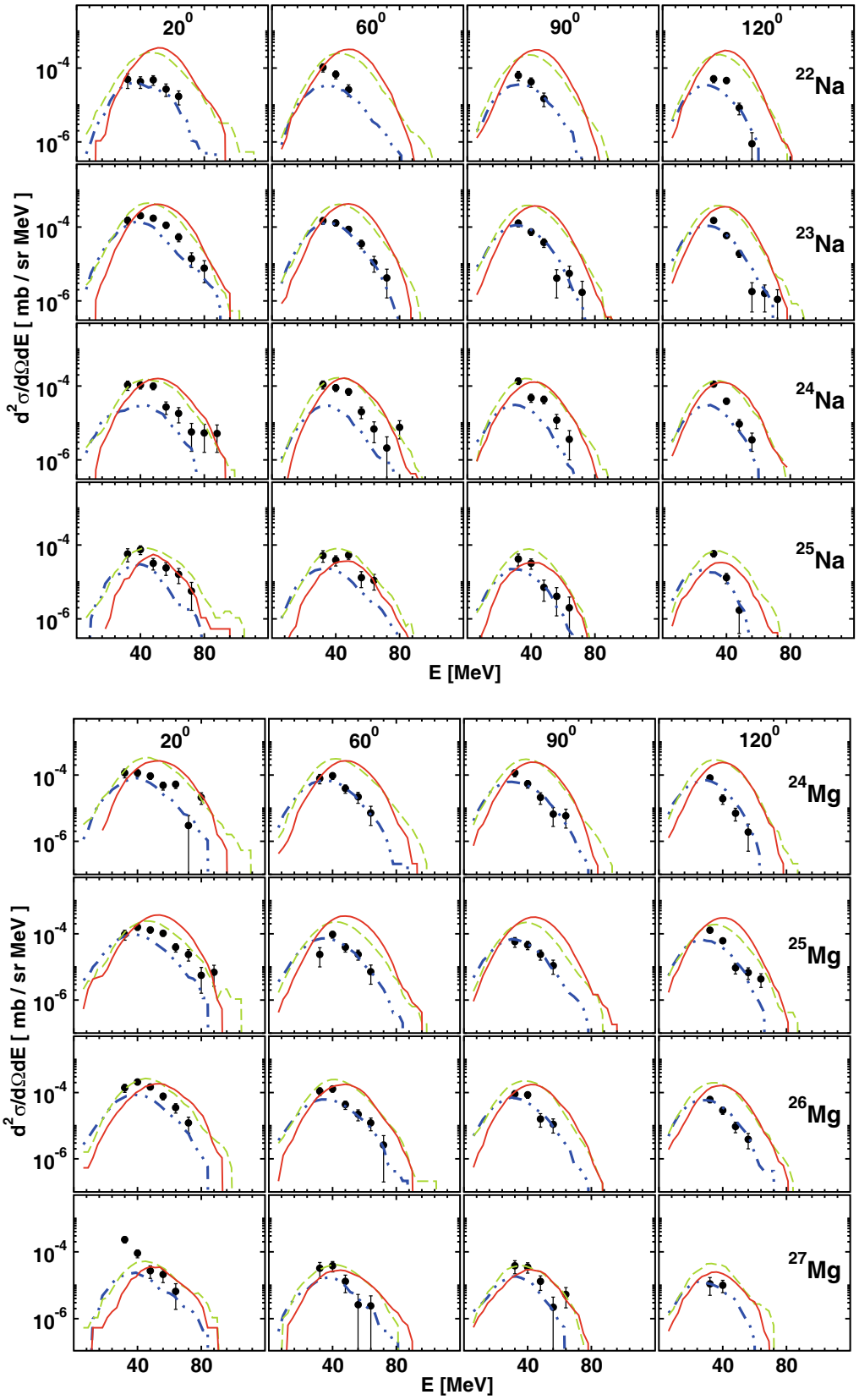

Fig. 5. Experimental (dots) and theoretical (lines) spectra for isotopes of Na (upper four panels) and Mg (lower four panels) emitted at four different angles: 20, 60, 90, and 120 degrees (columns from left to right). The lines: solid (red), dashed (green), dash-dotted (blue) and dotted (yellow) correspond to SMM, ABLA07, GEMINI++ and GEM2, respectively.

has the expectation value equal to zero and the standard deviation equal to unity. Values of the normal random variable are concentrated with probability 0.9973 inside the range of three standard deviations around its expectation value. Therefore in the case of perfect agreement of the calculated and experimental cross-sections, *i.e.*, when the model can be validated, absolute values of the standardized H and M deviation factors should be almost certainly smaller than 3.0.

The standardized values of the H- and M-factors were evaluated for all data shown in figs. 1–5 and for four theoretical models discussed above. These values are depicted in fig. 6 where four upper panels represent the H deviation factor and four lower panels correspond to the M deviation factor. Each of these four panels contains the deviation factors calculated by means of different theoretical models: GEMINI++,GEM2, ABLA07 and SMM in clockwise direction. Calculations for different elements are presented by different symbols and isotopes of the same element are connected by solid lines. The dashed (yellow) area represents H and M values smaller than 3.0, *i.e.*, it corresponds to the perfect agreement between the experimental and calculated cross-sections.

The factors decrease in average with the mass of ejectile what may be explained by the fact that the cross-sections for lighter ejectiles are significantly larger than those for heavier ones thus the corresponding relative statistical errors in formulae (1) and (2) are smaller. The GEM2 model produces larger deviation factors for light IMF than the other models. The H and M deviation factors evaluated with GEM2 cross-sections are not shown in fig. 6 for IMF with mass larger than 22. This is because the cross-sections calculated by GEM2 for heavy IMF are significantly smaller than the data (and therefore with large statistical error of Monte Carlo calculations). Such a model mass dependence of the yield is in quantitative as well as qualitative disagreement with that of the data.

The monotonic decrease of the H- and M-factors with mass of isotopes of each element of heavy IMF is clearly visible. Their values for light isotopes are significantly out of the range of validation of the models but they almost approach it for the heaviest isotopes. This mass dependence may be traced to systematic overestimation of the data by ABLA07 and SMM for lightest isotopes of each element.

The deviation factors evaluated with GEMINI++ do not show such monotonic behavior, what may be caused by different physical picture of the de-excitation of the target residuum by GEMINI++ (sequential emission of IMF) than that offered by ABLA07 and SMM (simultaneous multifragmentation).

Values of the deviation factors for GEMINI++ are the smallest among all four models. They approach the validation region (yellow band in fig. 6) for Ne, Na and Mg isotopes. Thus, the quantitative investigation of the quality of data reproduction seems to support conclusions from the qualitative considerations.

The quantitative analysis shows that only the data for heaviest products, *i.e.* isotopes of Ne, Na and Mg are satisfactorily well reproduced by theoretical models with the GEMINI++ being superior in respect to other models. The ABLA07 and SMM models seem to produce an equivalent description of the data whereas the GEM2 the worst one. The deviation factors do not discriminate automatically the GEM2 model, however, its predictions concerning the mass dependence of the yield of IMF are in qualitative disagreement with the data. This indicates that the physical conclusions cannot exclusively rely on the examination of the deviation factors even if they grant the objective measure of the agreement between the data and cross-sections as calculated by the models.

In the following step of the analysis the ranking of the description of the data by the studied models was performed. It was done taking into account the fact that the "perfect" agreement was achieved only for small set of the products —the heaviest IMF. The ranking was based on values of the deviations factors —separately for the H-factor and the M-factor. In the case when different models produced the same values of the deviation factors in the limits of errors the tied rank was calculated as the average of individual ranks. Results of the analysis are presented in table 1. As can be seen the ranks of the models estimated from the H-factor and M-factor are practically identical with only few exceptions. On the other hand ranks of different models vary from ejectile to ejectile. To assure some general ranking the sum of ranks of each model for different reaction products has been calculated and is shown at the bottom of the table.

As can be seen the sum of ranks is the smallest for GEMINI++. It is about 10%, 25% and 70% larger for SMM, ABLA07 and GEM2, respectively. This result is in agreement with the conclusions which state that the GEMINI++ offers the best description, SMM and ABLA07 give almost the same results, slightly poorer than GEMINI++, and GEM2 description is the worst.

3 Summary

The double-differential cross-sections $\mathrm{d}^2\sigma/\mathrm{d}\Omega\,\mathrm{d}E$ measured by Green *et al.* [5] for isotopes of ten elements (from Li to Mg) emitted from $\mathrm{p} + \mathrm{Ag}$ collisions at a proton beam energy of 480 MeV were analyzed using a microscopic two-step model. The first step of the reaction was described by the intranuclear cascade model INCL4.6 [13] and the second step by four models (ABLA07 [14], GEMINI++ [15, 16], GEM2 [17, 18] and SMM [19–22]) which realize different scenarios of the de-excitation of the equilibrated target remnant. The quality of agreement between the data and model cross-sections was judged on the basis of values of two deviation factors: the H-factor [28] and the M-factor [29]. It was found that the best, *i.e.*, the smallest values of these factors were obtained by the GEMINI++ model for the heaviest ejectiles. The absolute value of standardized H- and M-factors was in this case small enough to claim that GEMINI++ is validated. However for light IMF the absolute values of the deviation factors were very large for all models. Thus none of them may be fully validated for all the reaction products.

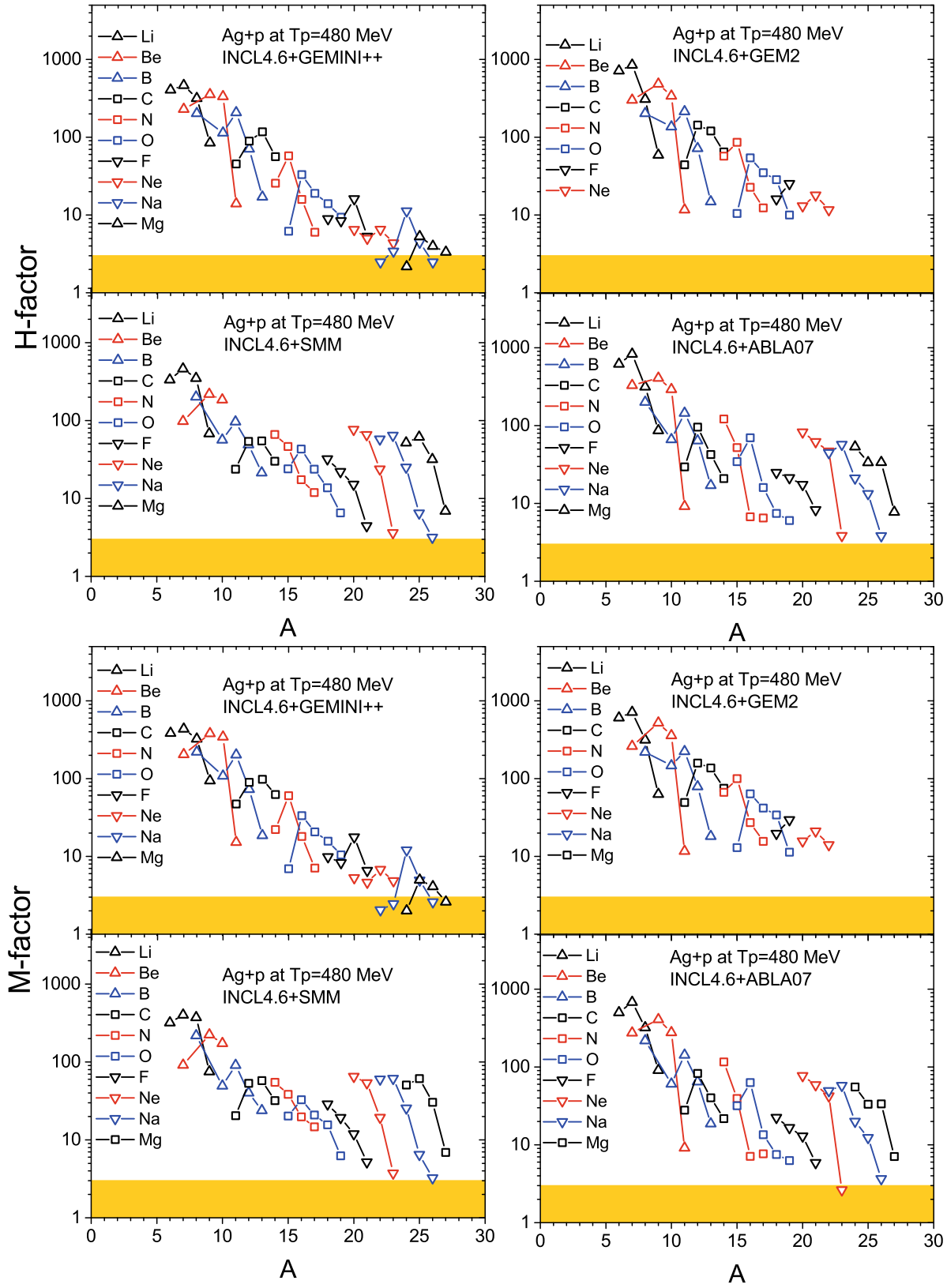

Fig. 6. Standardized values of the H-factor (four upper panels) and of the M-factor (four lower panels) for all intermediate mass fragments presented as a function of their mass number. Values of the H- and M-factors evaluated for different isotopes of the same element are depicted by the same symbols and are connected by solid lines. Individual panels of the figure correspond to intranuclear cascade calculations performed with the INCL4.6 model coupled to four different models describing the second stage of the reaction (GEMINI++, GEM2, ABLA07, and SMM in clockwise direction).

Table 1. Ranks of various model predictions for IMF spectra from p + Ag collisions at 480 MeV [5] according to the values of standardized H and M deviation factors taking into account both experimental and Monte Carlo uncertainties.

	Standardized H				Standardized M			
Ejectile	ABLA	GEM2	GEMINI	SMM	ABLA	GEM2	GEMINI	SMM
^{6}Li	3	4	2	1	3	4	2	1
^{7}Li	3	4	2	1	3	4	2	1
^{8}Li	2.5	1	2.5	4	2	1	3	4
^{9}Li	4	1	3	2	3	1	4	2
^{7}Be	4	3	2	1	4	3	2	1
^{9}Be	3	4	2	1	3	4	2	1
^{10}Be	2	4	3	1	2	4	3	1
^{11}Be	1	2	3	4	1	3	2	4
^{8}B	2.5	2.5	2.5	2.5	2.5	2.5	2.5	2.5
^{10}B	2	4	3	1	2	4	3	1
^{11}B	2	4	3	1	2	4	3	1
^{12}B	2	4	3	1	2	4	3	1
^{13}B	2.5	1	2.5	4	2.5	1	2.5	4
^{11}C	2	3	4	1	2	4	3	1
^{12}C	3	4	2	1	2	4	3	1
^{13}C	1	4	3	2	1	4	3	2
^{14}C	1	4	3	2	1	4	3	2
^{14}N	4	2	1	3	4	3	1	2
^{15}N	2	4	3	1	1	4	3	1
^{16}N	1	4	2	3	1	4	2	3
^{17}N	2	4	1	3	1.5	3.5	1.5	3.5
^{15}O	4	2	1	3	4	2	1	3
^{16}O	4	3	1	2	3.5	3.5	1.5	1.5
^{17}O	1	4	2	3	1	4	2	3
^{18}O	1	4	3	2	1	4	2.5	2.5
^{19}O	1.5	4	3	1.5	1.5	3.5	3.5	1.5
^{18}F	3	2	1	4	3	2	1	4
^{19}F	2.5	4	1	2.5	2	4	1	3
^{20}F	3	4	2	1	1.5	4	3	1
^{21}F	3	4	2	1	4	2	1	3
^{20}Ne	3	4	1	2	4	2	1	3
^{21}Ne	3	2	1	4	4	2	1	3
^{22}Ne	4	2	1	3	4	2	1	3
^{23}Ne	1.5	4	3	1.5	1	4	3	2
^{22}Na	2	4	1	3	2	4	1	3
^{23}Na	2	4	1	3	2	4	1	3
^{24}Na	2	4	1	3	2	4	1	3
^{25}Na	3	4	1	2	3	4	1	2
^{26}Na	3	4	1.5	1.5	3	4	1.5	1.5
^{24}Mg	3	4	1	2	3	4	1	2
^{25}Mg	2	4	1	3	2	4	1	3
^{26}Mg	3	4	1	2	3	4	1	2
^{27}Mg	3	4	1	2	3	4	1	2
Sum of ranks	107	146.5	84.0	92.5	103.5	145	85.5	96
Final rank	3	4	1	2	3	4	1	2

In the next step of the analysis a ranking of the models was done on basis of the relative values of deviation factors obtained for different models. It turned out that the sum of ranks over all observed reaction products was the smallest for GEMINI++. The SMM and ABLA07 models had 10% and 25% larger sum of ranks, respectively, whereas the GEM2 model got 70% larger sum of ranks. This indicates that the physical assumptions of the GEM2 model are not well fulfilled, *i.e.*, the evaporation of particles from the equilibrated remnant of the target is not the only process of its de-excitation. The ABLA07 and SMM allow also for simultaneous multifragmentation of the excited nucleus whereas GEMINI++ treats multifragmentation as a sequential emission of particles traversing the specific barrier.

The inspection of figs. 1–5 allows to observe a systematic deviation of the model predictions from the data. It is largest for light IMF and decreases with their mass number being however visible for almost all ejectiles at forward scattering angles. Such a qualitative behavior is characteristic for non-equilibrium processes. The authors of the INCL4.6 tried to describe them assuming the surface coalescence of the target nucleons together with the nucleons escaping from the intranuclear cascade for IMF with the mass number $A < 9$ [13]. The present analysis shows that this model is not able to reproduce the observed effects for ^{6,7,8}Li and ^{7}Be. The slope of the theoretical spectra is too small what results in the overestimation of the high-energy tail of the experimental spectra.

It may be conjectured that the contribution of non-equilibrium processes should be added incoherently with that of equilibrium ones. Therefore the theoretical cross-sections of the equilibrium processes should be not larger than the experimental data. In the present analysis this condition is fulfilled only by GEM2 and GEMINI++ models. Since the GEM2 cross-sections are unrealistically small, the GEMINI++ model offers the only acceptable description of the equilibrium processes for the studied nuclear system. The contribution of non-equilibrium processes is necessary for the satisfactory reproduction of all the studied data with the exception of the heaviest IMF where the GEMINI++ describes well the experimental cross-sections.

We thank the code developers and authors A. Boudard, J. Cugnon, J.C. David, S. Leray and D. Mancusi for providing us with the latest version of their Liège intranuclear cascade code INCL4.6. We are also grateful A. Kelić-Heil for the improved version of ABLA07. One of us (SKS) gratefully acknowledges the support by the Foundation for Polish Science - MPD program, co-financed by the European Union within the European Regional Development Fund.

References

1. A.M. Poskanzer, G.W. Butler, E.K. Hyde, Phys. Rev. C **3**, 882 (1971).
2. E.K. Hyde, G.W. Butler, A.M. Poskanzer, Phys. Rev. C **4**, 1759 (1971).
3. G.D. Westfall, R.G. Sextro, A.M. Poskanzer, A.M. Zebelman, G.W. Butler, E.K. Hyde, Phys. Rev. C **17**, 1368 (1978).
4. R.E.L. Green, R.G. Korteling, Phys. Rev. C **22**, 1594 (1980).
5. R.E.L. Green, R.G. Korteling, K.P. Jackson, Phys. Rev. C **29**, 1806 (1984).
6. R.E.L. Green, R.G. Korteling, J.M. DAuria, K.P. Jackson, R.L. Helmer, Phys. Rev. C **35**, 1341 (1987).
7. A. Letourneau, A. Böhm, J. Galin, B. Lott, A. Péghaire, M. Enke, C.-M. Herbach, D. Hilscher, U. Jahnke, V. Tishchenko, D. Filges, F. Goldenbaum, R.D. Neef, K. Nünighoff, N. Paul, G. Sterzenbach, L. Pieńkowski, J. Tõke, U. Schröder, Nucl. Phys. A **712**, 133 (2002).
8. C.-M. Herbach, D. Hilscher, U. Jahnke, V.G. Tishchenko, J. Galin, A. Letourneau, A. Péghaire, D. Filges, F. Goldenbaum, L. Pieńkowski, W.U. Schröder, J. Tõke, Nucl. Phys. A **765**, 426 (2006).
9. A. Bubak, A. Budzanowski, D. Filges, F. Goldenbaum, A. Heczko, H. Hodde, L. Jarczyk, B. Kamys, M. Kistryn, St. Kistryn, St. Kliczewski, A. Kowalczyk, E. Kozik, P. Kulessa, H. Machner, A. Magiera, W. Migdał, N. Paul, B. Piskor-Ignatowicz, M. Puchała, K. Pysz, Z. Rudy, R. Siudak, M. Wojciechowski, P. Wüstner, Phys. Rev. C **76**, 014618 (2007).
10. A. Budzanowski, M. Fidelus, D. Filges, F. Goldenbaum, H. Hodde, L. Jarczyk, B. Kamys, M. Kistryn, St. Kistryn, St. Kliczewski, A. Kowalczyk, E. Kozik, P. Kulessa, H. Machner, A. Magiera, B. Piskor-Ignatowicz, K. Pysz, Z. Rudy, R. Siudak, M. Wojciechowski, Phys. Rev. C **78**, 024603 (2008).
11. A. Budzanowski, M. Fidelus, D. Filges, F. Goldenbaum, H. Hodde, L. Jarczyk, B. Kamys, M. Kistryn, St. Kistryn, St. Kliczewski, A. Kowalczyk, E. Kozik, P. Kulessa, H. Machner, A. Magiera, B. Piskor-Ignatowicz, K. Pysz, Z. Rudy, R. Siudak, M. Wojciechowski, Phys. Rev. C **80**, 054604 (2009).
12. A. Budzanowski, M. Fidelus, D. Filges, F. Goldenbaum, H. Hodde, L. Jarczyk, B. Kamys, M. Kistryn, St. Kistryn, St. Kliczewski, A. Kowalczyk, E. Kozik, P. Kulessa, H. Machner, A. Magiera, B. Piskor-Ignatowicz, K. Pysz, Z. Rudy, R. Siudak, M. Wojciechowski, Phys. Rev. C **82**, 034605 (2010).
13. A. Boudard, J. Cugnon, J.-C. David, S. Leray, D. Mancusi, Phys. Rev. C **87**, 014606 (2013).
14. A. Kelić, M.V. Ricciardi, K.-H. Schmidt, *Proceedings of the Joint ICTP-IAEA Advanced Workshop on Model Codes for Spallation Reactions, ICTP Trieste, Italy, 4-8 February 2008*, edited by D. Filges *et al.* (IAEA, Vienna, 2008) IAEA INDC(NDS)-530, p. 181, `http://www-nds.iaea.org/reports-new/indc-reports/indc-nds/indc-nds-0530.pdf`, arXiv:0906.4193 [nucl-th].
15. R.J. Charity *et al.*, Nucl. Phys. A **483**, 371 (1988).
16. R.J. Charity, Phys. Rev. C **82**, 014610 (2010).
17. S. Furihata, Nucl. Instrum. Methods B **171**, 251 (2000).
18. S. Furihata, T. Nakamura, J. Nucl. Sci. Technol. Suppl. **2**, 758 (2002).

19. A.S. Botvina, A.S. Iljinov, I.N. Mishustin, Sov. J. Nucl. Phys. **42**, 712 (1985).
20. A.S. Botvina, A.S. Iljinov, I.N. Mishustin, J.P. Bondorf, R. Donangelo, K. Sneppen, Nucl. Phys. A **475**, 633 (1987).
21. A.S. Botvina, A.S. Iljinov, I.N. Mishustin, Nucl. Phys. A **507**, 649 (1990).
22. J.P. Bondorf, A.S. Botvina, A.S. Iljinov, I.N. Mishustin, K. Sneppen, Phys. Rep. **257**, 133 (1995).
23. V.F. Weisskopf, D.H. Ewing, Phys. Rev. **57**, 472 (1940).
24. F. Atchison, *Jül-conf-34: Proceedings of the Meeting on Targets for Neutron Beam Spallation Source, KFA-Jülich, Germany, June 1979* (1980) p. 17.
25. W. Hauser, H. Feshbach, Phys. Rev. **87**, 366 (1952).
26. N. Bohr, J.A. Wheeler, Phys. Rev. **56**, 426 (1939).
27. L.G. Moretto, G.J. Wozniak, Prog. Part. Nucl. Phys. **21**, 401 (1988).
28. A.Yu. Konobeyev *et al.*, J. Korean Phys. Soc. **59**, 927 (2011).
29. S.K. Sharma, PhD Thesis, Jagiellonian University (2015).